PAPER • **OPEN ACCESS**

Equilibrium, kinetic and thermodynamic analysis petroleum oil adsorption from aqueous solution by magnetic activated carbon

To cite this article: T H Nazifa *et al* 2019 *IOP Conf. Ser.: Mater. Sci. Eng.* **495** 012060

View the article online for updates and enhancements.

IOP ebooks™

Bringing you innovative digital publishing with leading voices to create your essential collection of books in STEM research.

Start exploring the collection - download the first chapter of every title for free.

This content was downloaded from IP address 124.207.82.166 on 18/09/2019 at 17:39

Equilibrium, kinetic and thermodynamic analysis petroleum oil adsorption from aqueous solution by magnetic activated carbon

T H Nazifa[1], T Hadibarata[2], A Yuniarto[3], M S Elshikh[4] and A Syafiuddin[1]

[1] Department of Water and Environmental Engineering, Universiti Teknologi Malaysia, 81310 UTM Skudai, Johor, Malaysia
[2] Department of Environmental Engineering, Curtin University, Malaysia, 98009 Miri Sarawak, Malaysia
[3] Department of Environmental Engineering, Faculty of Civil, Environmental and Geo Engineering, Institut Teknologi Sepuluh Nopember, 60111 Surabaya, Indonesia
[4] Botany and Microbiology Department, King Saud University, 11451 Riyadh, Saudi Arabia

[a]Corresponding author: hadibarata@curtin.edu.my

Abstract. A potential magnetized adsorbent was developed by a simple chemical process using iron oxide and banana stem based activated carbon for the treatment of petroleum oil. For batch experiment, pH (2-10), adsorbent dose (0.5 g/L -15 g/L), initial concentration (200-4500 ppm), agitation (50-150 rpm), temperature (25-45 ^{o}C) parameters were investigated. XRD, FTIR and FESEM analysis confirm the significant reflux of iron particles on prepared magnetic activated carbon. Data analysis calculated a removal of more than 95% at 1000 ppm petroleum oil within first 30 min of contact time. Freundlich, Langmuir, Temkin and Dubinin Radushkevich isotherm models were studied. The obtained data was found to fit well with Pseudo second order kinetic model and Freundlich isotherm model with a good correlation factor (R^2) of 0.9998 and 0.9914, respectively. Thermodynamic parameters expressed the exothermic nature of the adsorption process and the result shows maximum adsorption capacity of 1.90 g/g (approx.) at 25 ^{o}C. The composite adsorbent shows a good oil adsorption capacity with rapid kinetics and able to be recovered along with adsorbed oil by applying an external magnet. Hence, the prepared adsorbent is proved to be an effective candidate for the fast removal of petroleum oil spills by magnetic separation.

1. Introduction

Aquatic system is under critical condition for over the past few decades because of massive spill accidents mainly caused by human carelessness and mistake whereas a small contribution comes from industrial effluents or by the machineries and pipe leakage into the water system. Oil drilling operation, collision involving oil tankers accident, runoffs from seaward oil exploration and production, and during fuel unloading and loading operation are also responsible for offshore &

Content from this work may be used under the terms of the Creative Commons Attribution 3.0 licence. Any further distribution of this work must maintain attribution to the author(s) and the title of the work, journal citation and DOI.
Published under licence by IOP Publishing Ltd

shoreline pollution [1]. These spill accidents affect human health condition, environmental eco system and needless to say a huge waste of petroleum energy [2]. Therefore, it earns a great concern to clean and collect the spilled oil as soon as possible after an incident occurred. Different techniques like skimmers, synthetic organophilic sorbent (silica aerogel, zeolite, organophilic clays, graphene framework, cellulose fibre etc.) have been widely used for oil removal. Now a day due to higher adsorption capacities, better biodegradability, and cost effectiveness, natural materials are applied largely in comparison with inorganic and synthetic materials. It was found that natural materials performance are closely comparable to those of synthetic materials [3,4,5,6,7,8].

In adsorption process, impurities or pollutants are removed by contact between fluid and solid adsorbent. Activated carbons are widely used in adsorption process for various oil pollution as well as waste water treatment. Nevertheless, its demerit is the huge cost of commercially produced activated carbons. Therefore, agricultural waste based activated carbon has been given priority recently since the significance of low cost activated carbon prepared from sustainable raw materials are growing [9]. One of the important characteristics that must be fulfilled by any adsorbent to be applied in mass scale for any environmental utilization are the recyclability, biocompatibility and efficiency. Although, a number of currently available adsorbent materials full fill these demands, after oil adsorption they experience a main disadvantage regarding the expulsion of adsorbent material along with adsorbed oil droplets from the water. Moreover, oil adsorption process is time consuming and tedious task since a large volume of oil need to be cleaned quite efficiently and quickly to prevent from further spreading. This kind of difficulty can be minimized by the addition of magnetic functionality on the adsorbent materials which simplify the quick recovery by the presence of an external magnet and thereby boosting the overall effectiveness of the adsorption process [10].

Iron oxide nanoparticles (γFe_2O_3 or Fe_3O_4) has been confirmed its lower level of toxicity even at considerably high dosage. This makes the nanoparticles of iron oxide as an excellent magnetic material in the fields like drug delivery, bio-diagnostic, MRI and also chosen as the magnetic constituent of the adsorbent materials [10]. Nevertheless, the synthesis process of these compounds includes comparatively complex procedures as well as costly chemicals with the low yield. Hence cost effectiveness for a bulk amount generation for real time application is not worthy. Relatively inexpensive natural sorbent compounds like epoxidized natural rubber, cellulose hydrogel, and collagen fibers chemically activated carbon derived from palm shell have been suggested to overcome these major concerns [11]. But they also experienced a minimum oil adsorption capacity or slow/gradual response time which deceases process efficiency. Therefore, a cheap and efficient adsorbent which can be applied in immediate action or sudden removal of oil spill accidents is still an open area of research.

Aligning the aforementioned research necessity, the present study aims to investigate the capability of activated carbon derived from banana stem (*Musa acuminata*) incorporated with iron nanoparticles as an adsorbent and evaluation of its kinetic, isotherm, and thermodynamic behaviors. The main reason to select banana stem as the carbon source in the present work is due to its availability and less cost which suggest the material an ideal source for large-scale production of activated carbon. A liquid phase activation was carried out before incorporation with iron nanoparticles to increase the porosity and surface area for increased oil adsorption capacity of prepared activated carbon at 400 ^{0}C.

2. Materials and method

2.1. Materials

Dry banana stems were collected from local market in Johor Bahru, Malaysia. Petroleum fuel was purchased from BHP Petrol station, Johor, Malaysia. The physio chemical properties of petroleum are given in Table 1. Iron(II) chloride, $ZnCl_2$, and ferrous sulphate was purchased from Qrec^{TM}, Malaysia. Other chemicals used in this experiment were of AR grade.

Table 1. Physiochemical characteristics of petroleum oil

Parameter	Properties
Structure	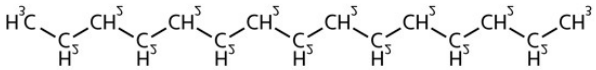
Molecular formula	$C_{10}H_{20}$ to $C_{15}H_{28}$
Appearance	Slightly brown viscous liquid
Molecular weight	178.6
Elemental analysis	carbon 85.9% (ww-1), hydrogen 13.1% (ww-1), nitrogen 0.3 % (ww-1)
Boiling point	180-360 °C
Aqueous solubility (15 °C)	0.005 g/L
Density	0.87 to 0.96 g/cm^3
Viscosity (cp)	604

2.2. Activated carbon production

Banana stems were cut into small portions and rinsed with distilled water to remove visible dirt and were oven dried at 105 ^{o}C. The dried samples were impregnated with $ZnCl_2$ in water by 1:1 ratio for 24 hours. After drying of impregnated banana stems, they were pyrolyzed at 400 ^{0}C under a constant nitrogen gas flow for 2 h. The pyrolyzed activated carbon was grounded and crushed to a fine powder form using mortar and pestle (sample code AC).

The prepared banana stem activated carbon was magnetized following previous procedure. The sample (AC; 30-40) g, was suspended in distilled water (500 mL). Freshly prepared ferric chloride solution mixed with ferrous sulphate solution and stirred vigorously at 80-90 ^{0}C. Aqueous suspension of AC then added with the ferrous and ferric chloride mixture. The combination is stirred slowly for 40 min. Finally, freshly prepared 10M NaOH was added drop by drop to make final pH of the mixture 10 to 11. The suspension was aged at 25 ºC temperature for one night and then reiteratively washed with de ionized water followed by ethanol. The magnetized activated carbon was dried overnight in an oven at 60 ^{0}C (sample code MAC).

2.3. Batch studies

The petroleum fuel was added with distilled water to make an artificial oil spill or oily waste water sample and agitated for few minutes for homogenous spreading of oil. Adsorption experiment was performed by adding 0.1 g of MAC in 250 ml erlenmeyer flask containing 100 ml of 1000 ppm oily water at pre-determined mixing rate. The pH (acidity) of the mixture was regulated using NaOH or 0.1M HCl. At an appropriate time interval, the samples were then withdrawn and adsorbents were separated from the working solution by external magnet followed by filter paper. Filtered oil water mixture was transferred in a separation funnel where equal volume of n-hexane is added. The mixture was agitated vigorously for 2 min and then kept at rest for 15 min for visible separation. After this, the solvent portion was slowly drained, and the extraction procedure was rerun for another two times. Finally, extracted volume of solvent is concentrated using rotary evaporator and washed with 10 ml hexane to inject 1 µL in GC-FID (Agilent 7820A, column type HP5, He flow rate is 3.0 ml/min). The oven parameter was started at 35 ºC initial temperature, hold for 2 min, then increased to a temperature at 290 ºC at a rate of 12 ºC/min. The oil content is measured for each specimen both prior and after

adsorption. Three duplicates of each test run were commenced, and mean value attained from replicates is taken for consideration to calculate the remaining oil content. Table 2 shows the summary of whole experiments in batch adsorption.

Table 2. Summarizes for all experiments of batch adsorption.

Parameters	Initial pH	Dosage (g)	Time (min)	Agitation (rpm)	Initial Concentration (mg/L)	Temp (K)
Effect of Initial pH	2 - 10	0.1 g	10	50	1000	298
Effect of Dosage	6.00	0.05 - 1.5	10	50	1000	298
Effect of Contact Time	6.00	0.2	5 - 70	50	1000	298
Effect of Agitation	6.00	0.2	30	50 - 150	1000	298
Effect of concentration	6.00	0.2	30	100	200 - 4500	298
Thermodynamic study	6.00	0.2	30	100	4500	298, 308, 318

Percentage removal of residue oil and adsorption capacity is calculated by the following equation:

$$\text{Removal rate (\%)} = \frac{C_0 - C_e}{C_0} \times 100 \quad (1)$$

$$\text{Adsorption Capacity} = q_e = \frac{(C_0 - C_e)V}{W} \quad (2)$$

Here, C_0 and C_e are the initial and final oil concentration (mg/L) before and after oil adsorption, W is the mass (g) of the adsorbent added in the V(volume) of solution (L).

The four isotherm studies were carried out in this study. The well-known Freundlich, Langmuir, Temkin, Dubinin-Radsuhkevich (D-R) isotherm models were applied to analyse the experimental result and their linear form of equations are given below:

$$\text{Langmuir equation} \quad \frac{C_e}{q_e} = \frac{1}{K_L q_m} + \frac{C_e}{q_m} \quad \text{w(3)}$$

$$\text{Freundlich equation} \quad \ln q_e = \ln K_F + \left(\frac{1}{n}\right) \ln C_e \quad (4)$$

$$\text{Temkin equation} \quad q_e = B \ln A + B \ln C_e \quad (5)$$

$$\text{Dubinin-Radsuhkevich} \quad \ln q_e = \ln q_D - \beta_D \left[RT . \ln\left(1 + \frac{1}{C_e}\right) \right] \quad (6)$$

where, q_e (mg/g) is the adsorbed oil, C_e (mg/L) is equilibrium oil concentration, K_L (L/mg) and qm (mg/g) expresses Langmuir constant and theoretical maximum adsorption capacity respectively. The 'n' and K_F are the Freundlich constant, which depicts the adsorption magnitude and the degree of non-linearity between the adsorption and concentration of the solution. A and B are Temkin constant. q_D

(mg/g) is the monolayer saturation capacity of adsorbent, β_D= Dubinin–Radushkevich isotherm constant (mol^2/kJ^2), R represent the universal gas constant which is 8.314 J/mol K, absolute temperature (K). In addition, Langmuir isotherm is expressed as R_L, it is a dimension less constant factor, can be expressed by following equation.

$$R_L = \frac{1}{1 + K_L C_o} \tag{7}$$

where C_0 denotes the initial concentration of oil. The values of R_L corresponding the isotherm types are shown in Table 3.

Table 3. The parameter R_L indicates the shape of isotherm as follows.

Value of R_L	Type of Isotherm
$R_L > 1$	Unfavourable
$R_L = 1$	Linear
$0 < R_L < 1$	Favourable
$R_L = 0$	Irreversible

The mean free energy per molecule (E) in the D-R model, is computed by the following equation:

$$E = \frac{1}{\sqrt{2\beta}} \tag{8}$$

Adsorption kinetics study is important for the aqueous effluent treatment analysis since it presents useful information regarding the adsorption mechanism. Three well established equations of pseudo first order, pseudo second order and intraparticle diffusion models were implied to find out the probable rate controlling states associated with petroleum oil adsorption, which are expressed by following linear equations respectively:

Pseudo-first-order model $$\ln(q_e - q_t) = \ln q_e + k_1 t \tag{9}$$

Pseudo-second-order model $$\frac{t}{q_t} = \frac{1}{K_2 q_e^{\,2}} + \frac{t}{q_e} \tag{10}$$

Intra-particle-diffusion $$q_t = k_{dif} t^{1/2} + C \tag{11}$$

where q_e and q_t (mg/g) respectively indicate the amount of BPA adsorbed at equilibrium and at time t (min); k_1 is the pseudo-first-order rate constant and k_2 is the pseudo-second order rate constant; k_t is the intraparticle diffusion rate constant (mg/g min$^{1/2}$) and C is the intercept which indicates the boundary layer thickness

2.4. Thermodynamic study

Thermodynamic parameters were assessed to affirm the adsorption nature. The effect of temperature (K) on petroleum adsorption onto MAC was studied over 25 to 45 ºC on 4500 mg/L oil concentration. Three basic thermodynamic parameters were investigated: the enthalpy change (ΔH°), entropy change (ΔS°) and free energy change (ΔG°). The free energy change (G°) was calculated by using the following equation

$$\Delta G° = -RT.\ln K_c \tag{12}$$

where, G° is the free energy change (J mol^{-1}), T is the absolute temperature (K), R is the universal constant (8.314 J mol^{-1} K^{-1}) and K_c is the thermodynamic equilibrium constant demonstrates the ratio between concentration of oil particles on adsorbent and in solution at equilibrium.

The relations between the enthalpy change (ΔH°), entropy change (ΔS°) and free energy change (ΔG°). The free energy change (ΔG°) were shown in the equation as follows:

$$\Delta G° = \Delta H° - T\Delta S° \tag{13}$$

Substituting and rearranging the ΔG◦ from Eq 12 gives the following equation:

$$\ln K_c = \frac{\Delta S°}{R} - \frac{\Delta H°}{RT} \quad (14)$$

where ΔH◦ and the ΔS◦ values were calculated from the slope and intercept of the linear plot of ln K_c and 1/T.

E_a (activation energy) defines the kinetic energy required by sorbate particles for the reactions with available active sites on adsorbent surface. The activation energy (E_a) can be calculated from Arrhenius equation as follows:

$$\ln K_c = \ln A - \frac{E_a}{RT} \quad (15)$$

A and E_a are the Arrhenius activation energy and factor. E_a value of 28.26 kJ mol^{-1} for petroleum was obtained by calculating the slope from the graph ln k_2 vs 1/T (1/K).

2.5. Characterization

Infrared spectra of the prepared AC and MAC were obtained using Fourier-transform infrared spectrometer (FTIR, Spectrum GX, Perkin Elmer, USA). The sampling was set up on KBr pellets and scanned over the range of 400-4000 cm^{-1} to determine the possible functional groups which are associated with adsorption. Surface morphology of AC and MAC was examined using a field-emission scanning electron microscope (FESEM, JEOL6335 F-SEM, Japan). X-ray diffraction (XRD) patterns for MAC were evaluated on a powder X-ray diffraction system using a Bruker D8 diffractometer system (Cu αradiation, 40 kV, 30 mA) for an angle 2θ between 5º to 90º.

3. Results and discussion

3.1. Characterization of adsorbents

The X-ray diffraction pattern of MAC is demonstrated in Figure 1. The magnetized phase referred to the maghemite (γ-Fe_2O_3) and magnetite (Fe_3O_4) formation since both materials are usually considered as magnetic materials. Moreover, the formation of γ-Fe_2O_3 and Fe_3O_4 is troublesome to distinguish by analysis. Both forms of iron oxide may show the same peak in the XRD pattern however, their properties are acceptable as both compound possesses magnetic phase [12]. The X-ray diffraction patterns display many sharp peaks which agrees with the presence of iron oxide. The major peaks were detected at 2Θ = 30.2º, 35.6º, 43.35º, 57.4º, 62.9º illustrate the domain of iron species exist as a crystalline form in prepared MAC sample. The observed peaks in the XRD pattern correspond to the peaks of Fe_3O_4 as evidenced from the comparison with the Fe_3O_4 simulated pattern. The average crystalline size of iron particles in MAC is found to be 10.29 nm by using Scherrer formula, D= 0.9λ/ B cosΘ [13]. Where D expresses the crystallite diameter, λ is the X-ray wavelength, Θ measures the Bragg angle, B denotes the width of the peak corrected for instrument broadening. The adsorption, hydrolysis and precipitation process are responsible to form these iron species onto MAC. The possible surface functional groups involved in adsorption of oil onto prepared MAC can be explained through infrared spectroscopy as shown in Figure 2. When compared to AC, additional band at 554 cm^{-1} on MAC correspond to the Fe_3O_4 nanocrystal, Fe-O vibration. The strong band at 3454 cm^{-1} in AC and 3434 cm^{-1} in MAC affirm the presence of bonded O-H groups of phenol or alcohol.

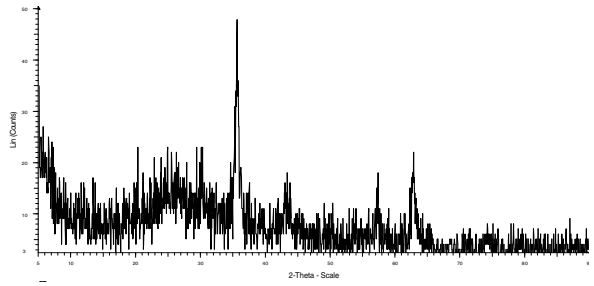

Figure 1. XRD pattern of magnetic activated carbon

The presence of amide group (C=O vibration band) was found at 1628 cm^{-1} in AC which after magnetization has shifted to 1620 cm^{-1}. However, a sharp peak at 1320 cm^{-1} suggests to the characteristic of C=C bonds of aromatic ring and peak at 782 cm^{-1} for C-C bonding, did not exhibit any shift. The existence of peaks both in AC and MAC at around 1000-1200 cm^{-1} represent the C-O functional group and related to holocellulose and lignin structures. Holocellulose is the mixture of cellulose and hemicellulose in the cell walls of plants [12].

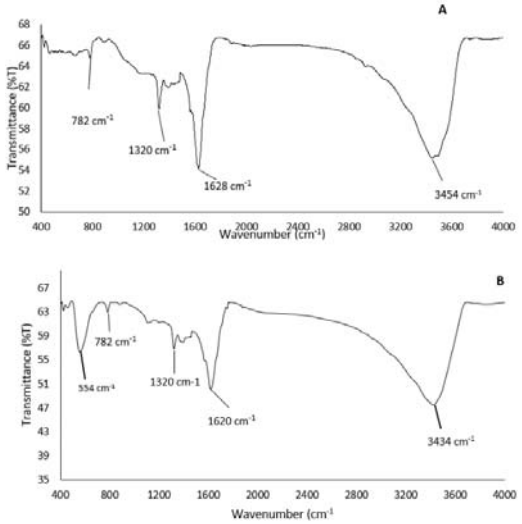

Figure 2. FTIR spectrum of Banana stem activated carbon (A); magnetic activated carbon of banana stem (B).

FESEM images of raw banana stem, banana stem activated carbon without $ZnCl_2$ impregnation and with $ZnCl_2$ impregnation and MAC before oil adsorption is shown in Figure 3. Micrograph of raw banana stem adsorbent and activated carbon without $ZnCl_2$ has been seen to be rough, valley like structure with less number of pores. However, after impregnation with $ZnCl_2$, banana stem activated carbon has developed a porous structure with small canals. Micrograph showed the morphological transformation due to FeO impregnation on the carbon matrix pores. Due to impregnation of iron species, the smooth surface of activated carbon has developed a spongy texture which is clearly observed on the MAC surface. Most of the carbon matrix cavities appear to possess iron nanoparticles. This well distributed iron particles are responsible for the blockage of some pores in MAC [14].

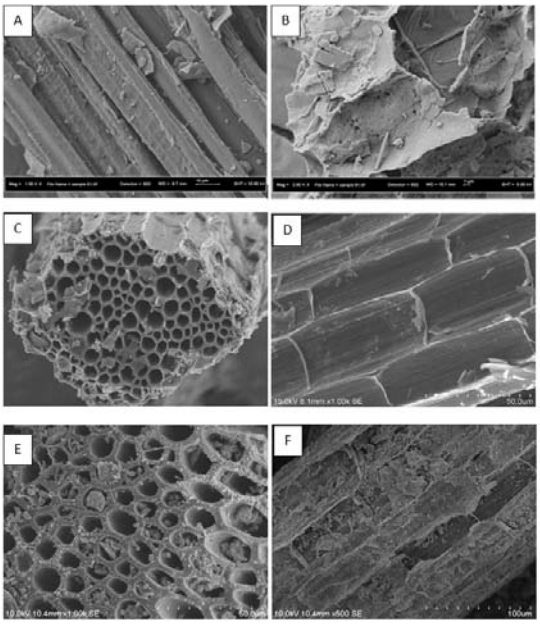

Figure 3. FESEM micrograph of raw banana stem (A), banana stem activated carbon (B), banana stem impregnated with $ZnCl_2$ activated carbon (C, D), magnetic activated carbon (E, F)

3.2. Batch studies

The effect of acidity was examined in the range of pH 2-10 as shown in Figure 4A. The acidity of the working solution was balanced by drop wise addition of 0.1M HCl and 0.1M NaOH. The percentage of removal and adsorption uptake has been increased dramatically from pH 2 to 6. At pH 2, adsorption capacity and percentage removal were found 700 mg/g and 70.1% which has been increased to a value of 868 mg/g and 86±1.1% at pH 6. At lower pH value, cationic properties of adsorbent surface have increased due to free protons available in the solution which increased the competition between oil molecules with H^+ ions and therefore responsible for lower adsorption capacity . There seen a minimal difference in adsorption capacity as well as removal percentage from pH 6 to 10 and the adsorption uptake was almost same from pH value 8 to 10 in the range of 855±1.4 to 893±1.21 mg g^{-1}. The reason can be explained like, as the pH increased the carbonyls present on the adsorbent turned to carboxylate anions. Approximately no changes in oil molecules removal was noticed after all carboxyl converted to carboxylate anions. Hence, the adsorption incremented when the acidic value of the working solution increased until the optimum [12]. pH 6 has been considered optimum for the rest of the experiment. Moreover, it suggests a supplementary preference in the treatment procedure since it falls within the range of sea water pH range (6-9) hence no further modification of pH will be needed after the adsorption process prior the effluent is ready to discharge. In any adsorption study binding sites associated with the adsorbent surface is reliant on pH value of solution [15].

The effect of agitation rate was analysed by adding 2 g/L adsorbent dose at pH 6 on 1000 mg/L mixture with varying mixing rate from 50 to 150 rpm for a contact time 30 min (Figure 4B). Both the value for removal efficiency (%) and adsorption uptake has increased slightly with the increased agitation speed. The removal percentage (97± 2.1) and adsorption uptake (487.5± 1.92 mg/g) showed maximum value at 100 rpm. As the speed increased, it facilitates more association between the adsorbent and petroleum oil. Further increased speed provides a declining trend of removal and adsorption uptake, due to higher velocity that promotes shearing of adsorbed oil.

The reaction mechanism that controls overall adsorption kinetics is linked with the initial oil molecules concentration in the sample. Figure 4C shows that adsorption of oil marked up with the increase of oil concentration. The percentage of removal of oil shows higher at lower initial petroleum

oil concentration at 200 mg/L and afterwards the removal percentage drops with the increment of initial concentration. However, the adsorption (mg/g) increased with the increase of initial oil concentration and attained its equilibrium state at concentration until 4000 mg/L. The equilibrium attained might be because of saturation of all active sites on the adsorbent surface. Lower concentration of oil has less number of hydrocarbon molecule to be adsorbed on adsorbent surface which results in lower adsorption uptake [2]. The oil water mixture was conducted with eight different quantity dosages of AC and MAC (Figures 4D & 4E). The removal percentage of oil or adsorption capacity was observed to be related with the application of both adsorbent. Maximum removal percentage was found at 2 g/L of MAC and 3 g/L of AC providing 94% and 80.3% removal of oil. As the amount of adsorbent application increases, more adsorption sites become available which induces a higher rate of removal. A further increase of MAC or AC dosage did not show any sharp increase to the removal percentage. In contrast, the adsorption take-up increased with the decrease of adsorbent dose addition. Maximal adsorption uptake was observed of 1342±1 mg g^{-1} for MAC and 760±0.8 mg for AC at 0.5 g/L dose. The gradient of concentration among adsorbent surface and adsorbates in the working solution is the cause for the decline of adsorption capacity with the increase of adsorbent dose.

3.3. Adsorption isotherm and kinetic

The data obtained from the research experiment showed that the increased dose of MAC induces a higher removal percentage of petroleum oil which proves magnetized activated carbon is an excellent adsorbent medium to treat petroleum oil spill treatment. However, limited information has been discussed in the literature on the adsorption of petroleum fuel in compare with the data derived from low molecular weight substances. Noteworthy information could be achieved over sorption isotherm. The isotherm fitted for Freundlich, Temkin, Langmuir and D-R model and the co efficient and values of the adsorption of petroleum oil onto MAC are shown in Table 4. The obtained data demonstrates an acceptable fit of Langmuir isotherm model to the experimental data with 0.9422 R^2 value.

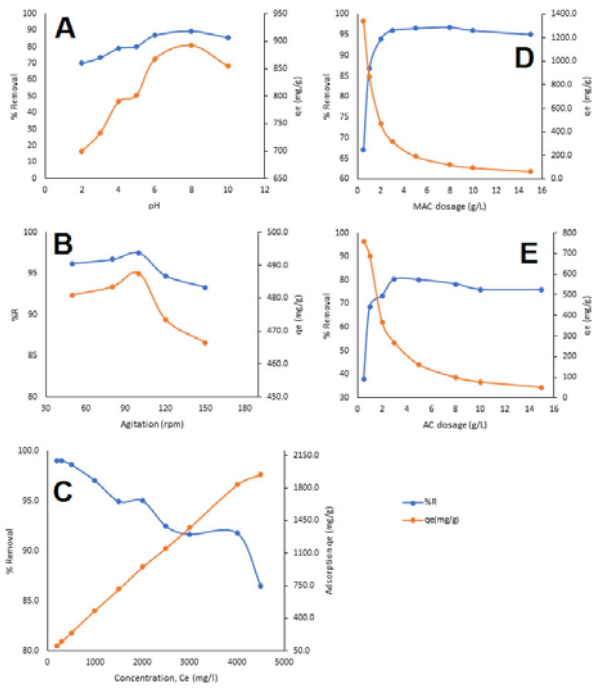

Figure 4. Effect of some parameters on adsorption of petroleum oil: pH (A), agitation (B), initial concentration (C) magnetic activated carbon dosage (D), activated carbon dosage (E).

Moreover, values of R_L shown in Table 5 suggests favourable adsorption of oil onto MAC. However, a higher value of R^2 equal to 0.9914 suggests that Freundlich isotherm model fits better for the petroleum oil adsorption onto MAC. Moreover, the value at $1< n < 10$ shows a favourable condition of adsorption and the estimated value of 'n' is greater than unity which is 1.935 for MAC. A higher K_F value 80.6 (L/gm) is an indicator of the good adsorption capacity.

Table 4. Comparison of Langmuir, Freundlich, Temkin and D-R isotherm model constant and correlation coefficient.

Isotherm	Parameter	Value
Langmuir	q_m (mg/g)	2000
	K_L (L/mg)	0.011
	R^2	0.945
Freundlich	K_F (mg g^- 1) (L mg^- 1)$^{1/n}$	80.6
	n	1.935
	R^2	0.9914
Temkin	A (L g^- 1)	0.353
	B	312.28
	R^2	0.8855
D-R Model	q_e (mg/g)	926.20
	B_D (mol^2 kJ^{-2})	3 x 10^{-6}
	R^2	0.6828
	E (KJ/mol)	0.408

However, lower R^2 value (0.8855) of Temkin model and that of D-R model (0.6828) depicts poor fitting between experimental data and isotherm equation. When the estimated value of E is below 8 kj/mol, then the process was defined as physical adsorption. On the other hand, the adsorption process was chemical adsorption when the value between 8-16 kJ/mol [16].

Table 5. R_L values based on Langmuir equation.

Co (mg/L)	R_L Values
200	0.3125
300	0.2325
500	0.153
1,000	0.0833
1,500	0.057
2,000	0.043
2,500	0.035
3,000	0.029
4,000	0.022
4,500	0.0198

Figure 5 indicated the estimated value of mean free energy is limited to 0.402. In light of this data, it can be inferred that the physical adsorption has played a controlling role in the adsorption procedure of petroleum oil adsorption onto MAC. The value of q_e (mg/g) and k for each kinetic model were estimated by plotting a graph ln (q_e-q_t) versus t, t/q_t versus t and qt versus $t^{1/2}$ for pseudo first order, second order and intraparticle diffusion.

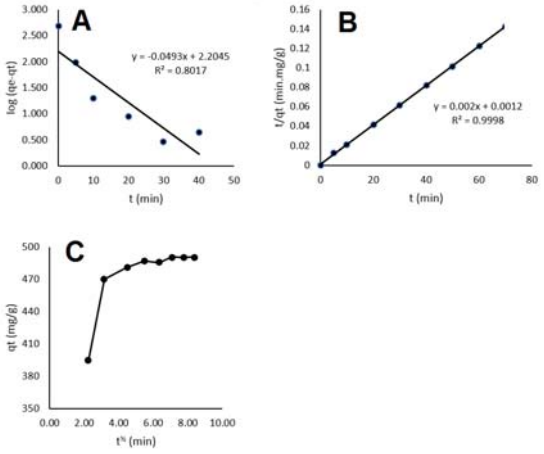

Figure 5. Kinetic studies of petroleum oil adsorption: Pseudo-first-order (A), pseudo-second-order (B) and intraparticle diffusion model (C).

In pseudo first order model, the plot shows linearity and the R^2 values are observed to be 0.8017, the calculated q_e values (q_1, calc.) are not in agreement with the experimental qe values (q_e exp). The result showed that the adsorption of petroleum oil was not a first-order kinetics. However, amount of adsorbed oil (mg/g) for experiment (q_e, exp) was similar with pseudo second order equation. Furthermore, R^2 value of 0.9998 was calculated from pseudo second order equation which proves to be better fit in compare to intraparticle diffusion and pseudo first order isotherm model.

3.4. Adsorption thermodynamic

Since the adsorption uptake of oil declined with the increase of temperature as provided in Figure 6, it indicates that the procedure was exothermic [2]. The oil adsorption capacity at 25 ℃ is approximately 1.94 g/g, which is higher than other previous adsorbent used for petroleum oil. The value of ΔH°, ΔG° and ΔS° are given in Table 6. ΔH° and ΔS° are calculated by the slope and intercept of the linear plot of ln K_c versus 1/T (Figure 7). The calculated ΔG° value of 298K, 308K, 318K were −10.67 kJ mol^{-1}, -11.036 KJ mol^{-1} and -11.394 KJ mol^{-1}.

Table 6. Thermodynamic parameters for the adsorption of oil onto MAC

Temperature (K)	q_e (mg g^{-1})	ΔGº (kj mol^{-1})	ΔHº (kj mol^{-1})	ΔSº (kj mol^{-1} k^{-1})	E_a (kj mol^{-1})
298	1945±14.89	-10.67			
308	1835±10.71	-11.03	-4.37	35.817	28.26
318	1751±21.23	-11.394			

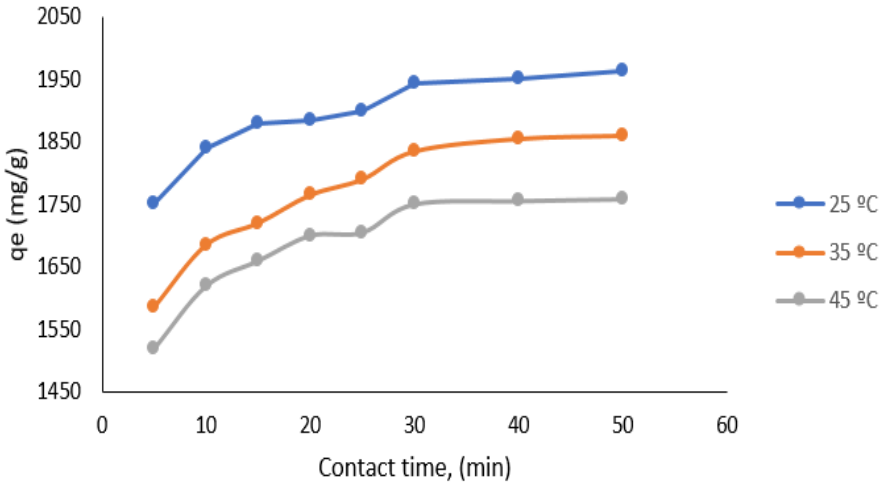

Figure 6. Thermodynamic study of petroleum oil adsorption onto magnetic activated carbon.

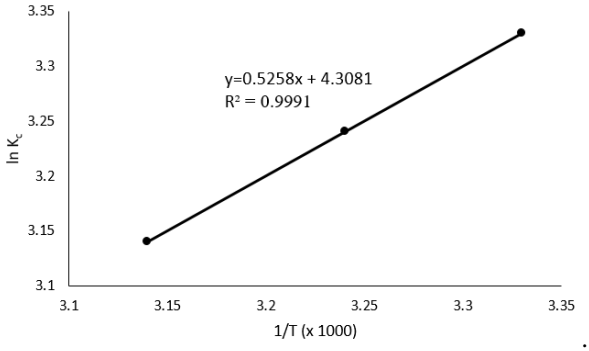

Figure 7. The plot between ln K_c versus 1/T for obtaining the thermodynamic parameters.

The negative values of ΔG° demonstrated that the adsorption procedure for the sample was possible & spontaneous thermodynamically. Nevertheless, the decrease in ΔG° values with increment of temperature demonstrated that the adsorption process was not favourable at higher temperatures [17]. The positive value for ΔS° indicated that the adsorption was not homogeneous. It indicates randomness of adsorption on solid/solution interface. The positive value of ΔS° may also occur due to redistribution of energy between adsorbent and adsorbate. The negative ΔH^{o} value confirmed that the exothermic tendency of adsorption process was supported by the decrease in oil uptake of the adsorbent with the ascent of temperature [17]. Normally, the activation energy for physical adsorption lies within 5 to 40 kj/mol while a higher range 40 to 80 KJ/mol denotes chemical adsorption. Hence the value of E_a (28.26 KJ/mol) exhibited that the adsorption mechanism was physical adsorption. A similar result was also found for the Acid Red 88 adsorption by magnetized $ZnFe_2O_4$ spinel ferrite nanoparticle [2].

4. Conclusion

A magnetized adsorbent was prepared from banana stem based activated carbon in corporation with iron oxide nanoparticles. The experiment demonstrated that the magnetic activated carbon is an attractive material for efficient oil spill treatment by external magnetic separation. In addition, the benefit of using banana stem as the sole carbon source is the availability of banana stem in Malaysia, Indonesia as well as other South East Asian countries. The successful $ZnCl_2$ impregnation onto AC

and magnetizing AC by iron oxide nanoparticles has increased its hydrophobicity, thus boosted the adsorption capacity.

FTIR, FESEM, and XRD analysis have explicated the significant precipitation of magnetic nanoparticles on AC. The adsorption of petroleum oil onto MAC followed pseudo second order kinetics and Freundlich isotherm model. Thermodynamic studies exhibited here expressed the exothermic nature and feasibility of the process, which is seen to be controlled by physiosorption process. Moreover, the separation of adsorbents by external magnet is less tiresome and spontaneous since magnetic particles interaction are engaged for the recovery of oil water mixture. This process can also be applicable for oil containment immediately after the spill to avoid further spreading. Finally, it can be say that, simplicity and cost effectiveness of this prepared MAC can be used as potential adsorbent for petroleum oil removal in conjugation with the current available technologies.

Acknowledgements
This research was a partially funded by a Fundamental Research Grant Scheme of Ministry of High Education Malaysia (No. 4F813) and Research Group Project of Deanship of Scientific Research, King Saud University (No RG -1435-086).

References

[1] Yang L, Wang Z, Li X, Yang L, Lu C and Zhao S 2016 *Water Air Soil Pollut.* **227** 346-358
[2] Sidik S, Jalil A, Triwahyono S, Adam S, Satar M and Hameed B 2012 *Chem. Eng. J.* **203** 9-18
[3] Hadibarata T, Syafiuddin A, Al-Dhabaan F A, Elshikh M S and Rubiyatno 2018 *Bioprocess Biosyst. Eng.* **41** 621-632
[4] Nikmatin S, Syafiuddin A, Hong Kueh A B and Maddu A 2017 *J. App. Res. Technol.* **15** 386-395
[5] Syafiuddin A, Salmiati, Hadibarata T, Kueh A B H and Salim M R 2018 *Nanomaterials* **8** 1-17
[6] Lazim Z M, Hadibarata T, Puteh M H, Yusop Z, Wirasnita R, Nor N M 2015 *Jurnal Teknologi* **74** 109–115
[7] Syafiuddin A, Salmiati S, Hadibarata T, Kueh A B H, Salim M R and Zaini M A A 2018 *Sci. Rep.* **8** 1-15
[8] Nor N M, Hadibarata T, Yusop Z, Lazim Z M 2015 *Jurnal Teknologi* **74** 117–122
[9] Sana D and Jalila S 2017 *Chin. J. Chem. Eng.* **25** 1282-1287
[10] Ali N, El-Harbawi M, Jabal A A and Yin C-Y 2012 *Environ. Technol.* **33** 481-486
[11] Ngarmkam W, Sirisathitkul C and Phalakornkule C 2011 *J. Environ. Manage.* **92** 472-479
[12] Zainol M M, Amin N A S and Asmadi M 2017 *Sains Malays.* **46** 773-782
[13] dos Santos T R T, Mateus G A P, Silva M F, Miyashiro C S, Nishi L, de Andrade M B, Fagundes-Klen M R, Gomes R G and Bergamasco R 2018 *Water Air Soil Pollut.* **229** 92-109
[14] Mohan D, Sarswat A, Singh V K, Alexandre-Franco M and Pittman Jr C U 2011 *Chem. Eng. J.* **172** 1111-1125
[15] Casagrande G C R, dos Reis C, Arruda R, de Andrade R L T and Battirola L D 2018 *Water Air Soil Pollut.* **229** 166-180
[16] Badruddoza A, Tay A, Tan P, Hidajat K and Uddin M 2011 *J. Hazard. Mater.* **185** 1177-1186
[17] Konicki W, Sibera D, Mijowska E, Lendzion-Bieluń Z and Narkiewicz U 2013 *J. Colloid Interface Sci.* **398** 152-160